J Mater Sci (2009) 44:5537–5543
DOI 10.1007/s10853-009-3775-2

On the essential work of fracture in polymer–metal multilayers

Géraldine Garnier · Béchir Chehab · Bernard Yrieix · Yves Bréchet · Lionel Flandin

Received: 20 April 2009 / Accepted: 22 July 2009 / Published online: 11 August 2009

Abstract Polyethylene terephtalate (PET) metallized with aluminium by physical vapour deposition was investigated through classical physical chemistry techniques and mechanical characterization. The amount of aluminium altered the amount of crystallinity of the PET substrate, but appeared unrelated to the mechanical properties obtained with regular tensile test. In contrast, the essential work of fracture (EWF), as obtained with Cotterell tests, permitted to better discriminate the perforation resistance. It is shown that increasing the amount of crystallinity within the PET linearly reduced the EWF.

Introduction

Polymer–metal multilayers have widely been used for decades in food packaging and, more recently, in building applications [8, 14]. These heterogeneous structures provide attractive combinations of properties involving mechanical resistance to perforation, barrier properties to air and water, weldability and low emissivity. This unusual set of properties make these materials especially well suited as envelopes for super thermal insulators used under vacuum for very long time. However, the issues of delamination resistance of these hybrid materials, in their initial state as well as after some ageing period, remain open.

Although more commonly employed by metallurgists, the essential work of fracture (EWF) method has already been used to characterize fracture for polymeric film. For example, this test has been applied to characterize the fracture behaviour of nanostructured polymer materials. Both the resistance against stable crack initiation and propagation are strongly sensitive to the morphology of the materials [11]. These tests were also used to determine the fracture toughness of polyethylene terephtalate (PET) and the maleated styrene/ethylene/butadiene/styrene copolymer (MA-g-SEBS) melt blended with PET [6]. In addition, Maspoch et al. [13] showed that the specific EWF is strongly affected by the orientation: w_e is greater in TD (perpendicular direction) than in MD (direction of extrusion). The authors proposed that this is due to a larger orientation of the films in TD than in MD. On the contrary, the non-essential or plastic work (βw_p, where β is the shape factor of the plastic zone) depends on the testing conditions [9]. Experimental results suggest that w_e is insensitive to microstructural changes within the polymer, whereas w_p is altered by their intrinsic properties.

Although the EWF method has been applied to polymer materials, there are no applications of this methodology, to our knowledge, to multilayers polymer–metallic films.

The aim of this study is to characterize quantitatively the mechanical properties and fracture resistance of metal polymer multilayers. Tensile tests allow to assess the classical mechanical parameters of the composites, but are not very discriminant as far as their fracture properties are concerned. The objective of this study is twofold (i) to demonstrate that the EWF method is also a discriminating

G. Garnier · B. Chehab · Y. Bréchet (✉)
SIMAP, Grenoble-INP, BP75, 1130 rue de la piscine,
38402 Saint Martin d'Hères, France
e-mail: ybrechet@ltpcm.inpg.fr; yves.brechet@grenoble-inp.fr

B. Yrieix
EDF R&D, Les Renardières, 77250 Moret sur Loing, France

G. Garnier · L. Flandin
LMOPS, UMR CNRS 5041, Université de Savoie, Bât IUT,
73376 Le Bourget du Lac, France

tool for polymer–metal films; (ii) to investigate the effects of structure on the fracture behaviour of multilayers films.

Materials and methods

Materials

To ensure the above-described multifunctional requirements for vacuum insulation, multilayer films must be composed of at least three principal layers [2]: (i) a polymeric film (PET or polypropylene, PP), used for its good mechanical properties, (ii) a metallic film (Al) for the ultra high resistance to permeation of atmospheric gases and water vapour, (iii) another polymeric layer (low density polyethylene, LDPE) for the weldability. This article focuses on bimaterial layers of PET covered with one or two aluminium layers of different thicknesses by physical vapour deposition. The base material is a biaxial-oriented PET film of 12 μm thickness. The interface properties between polymer and aluminium coatings are expected to alter the final properties [2]; therefore, in order to improve the adhesion between polymer and metallic layers, two surface treatments before the deposition of the metallic coating were performed:

- In the so-called "chemical treatment", an acrylic coating (thin layer) is applied on one or two sides of the polymer.
- In the "corona treatment", the polymer being treated is exposed to an electrical discharge. Oxygen molecules within the discharge area break into their atomic form and are free to bond to the ends of the molecules in the material being treated, resulting in a chemically activated surface.

These materials were provided by the Rexor Company (Rexor, Paladru, France) from the same batch of PET 12 μm (Fig. 1, Table 1).

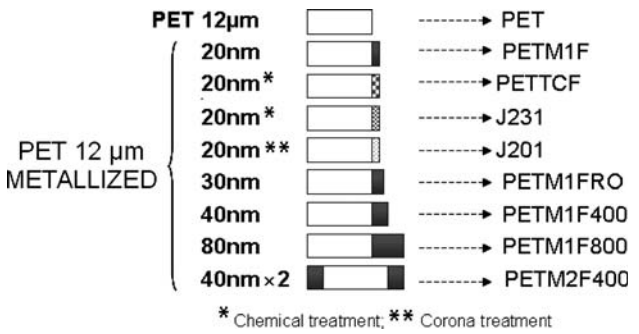

Fig. 1 Structure and schematic representation of polymer–metal films

Experimental method

Differential scanning calorimetry

The measurements were carried out on a DSC-7 instrument (PerkinElmer SAS, Courtaboeuf Cedex, France). All samples were cut off from foils in the form of small discs with a diameter of 7 mm. The instrument was calibrated with indium standard ($T_m = 156.6$ °C; $\Delta H_m = 28.4$ J/g). The reference was an empty aluminium pan and the average mass of samples was 5 mg (ten samples by pans). The samples were heated from 40 to 300 °C at a scan rate of 10 °C/min and then continued at a negative scan until the initial temperature was reached.

Thermal analyses were classically performed to identify the transitions occurring within the polymer layer. In the case of quenched PET, three transition temperatures may be observed during the first heating ramp namely the glass transition temperature (T_g), the cold crystallization temperature (T_{cc}) and the melting temperature (T_m) [10]. Below the glass transition temperature, the PET is in a glassy state with a very slow molecular mobility. Above the glass transition temperature, the mobile amorphous component becomes rubbery, meaning much more mobile. This increased mobility allows at a slightly higher temperature the material crystallization. At much higher temperature, the polymer will melt. All these events strongly depend on the state of crystallization of the polymer. The amount of semi-crystalline phase in PET could be determined with the integrated signal of the melting peak. Since the major contribution to the enthalpy of melting comes from the crystalline phase, the area of this peak is proportional to the fraction χ_c of crystalline polymer, as given by Eq. 1.

$$\chi_c = \Delta H_m / \Delta H_m^{\infty}, \quad (1)$$

where ΔH_m is the enthalpy of the polymer–metal composites and ΔH_m^{∞} is the enthalpy of completely crystalline PET. The value of ΔH_m^{∞} for PET found in the literature is 125 J/g [7].

Field emission gun scanning electron microscope

Scanning electron microscope (SEM) observations were performed with a ZEISS Ultra 55 SEM to analyse the structure of the aluminium layer. The presence of numerous heterogeneities was revealed that can be differentiated in two types according to their gray level. White spots could be identified as aluminium-rich phase, either heterogeneous aluminium deposition or more likely alumina particles. Dark spot could further be identified by energy dispersive X-ray analysis as lacks of aluminium in the layer. The typical size of the holes was close to 100 nm and their surface fraction varied from one film to the next.

Table 1 Designation and characteristics of the specimens used

Films	Abbreviations	Aluminium thickness (nm)	Treatment
PET reference (12 μm of thickness)	PET 12 μm	–	–
PET metallized on one side with 20 nm of aluminium	PETM1F	20	–
PET metallized on one side with 20 nm of aluminium	PETTCF	20	Chemical
PET metallized on one side with 20 nm of aluminium	J231	20	Chemical
PET metallized on one side with 20 nm of aluminium	J201	20	Corona
PET metallized on one side with 30 nm of aluminium	PETM1FRO	30	–
PET metallized on one side with 40 nm of aluminium	PETM1F400	40	–
PET metallized on one side with 80 nm of aluminium	PETM1F800	80	–
PET metallized on two sides with 40 nm of aluminium	PETM2F400	2 × 40	–

Measured defect densities for available evaporated aluminium coatings on PET ranging from 55 to 950 mm^{-2}.

Tensile tests

In order to characterize the resistance of fracture of the composites, tensile tests were performed using an universal testing machine, Adamel Lhomargy, equipped with a 100-N load cell and a grip-to-grip separation of 60 mm. Tests were conducted at a constant crosshead rate of 50 mm/min at room temperature until total failure of the specimens occurred. Dumb-bell specimens (5 mm in width and 30 mm in length) were cut in the machine direction according to NF ISO 6239. The tensile energy to fracture was calculated from the stress–strain curves; this parameter corresponds to the area under the curve.

Cotterell test

The EWF concept was introduced by Cotterell and Reddel [4] as a mean of quantifying the fracture resistance of thin ductile metal sheets.

The aim of the method is to separate, based on dimensional considerations, the work performed within the plastic zone (gross plasticity) from the total work of fracture in order to provide an estimate of the work spent per unit area within the fracture process zone (FPZ) to break the material [1]. If the ligament of a sheet specimen is completely yielded before initiation, and the plastic zone is confined to the ligament, then the plastic work performed for the complete fracture is proportional to the plastic volume at initiation and the work performed in the FPZ is proportional to the fracture area, i.e. the plastic work and the EWF scale differently with sample dimensions. For thin sheets, the double edge notch tension (DENT) geometry [3] is particularly adapted since the transverse stress between the notches is tensile and this geometry avoids buckling problems. The area of the plastic zone and the plastic work performed to completely fracture the specimen is proportional to the ligament, l_0, squared. The work performed in the FPZ is proportional to l_0. The total work of fracture, W_f, can be written as the sum of the essential work, W_e, and the plastic work, W_p,

$$W_f = W_e + W_p = t_0 l_0 w_e + \alpha t l_0^2 w_p, \quad (2)$$

where w_e is the specific EWF (work per unit area), w_p is an average plastic work density, t_0 is the initial sheet thickness, t is the specimen thickness and α is a shape factor. The specific work of fracture, $w_f = W_f/t_0 l_0$, is given by

$$w_f = w_e + l_0 \alpha w_p. \quad (3)$$

Thus, if a series of specimens with different ligament lengths is tested, the specific essential work is the constant term in the linear regression of the specific work of fracture against ligament length, i.e. the work obtained by extrapolating the linear evolution to a zero ligament length [12].

For the measurements of the EWF, DENT specimens with a thickness of 12 μm and with various ligament lengths (2–16 mm) were tested at room temperature under uniaxial tension at a crosshead rate of 50 mm/min using a universal testing machine. The DENT specimens present a total length, L, of 100 mm and a width, W, of 50 mm. All specimens were cut from rectangular shape in the longitudinal direction (machine direction). Initial notches were made perpendicularly to the traction direction with a fresh razor blade. So, a set of 24 specimens with varying ligament length has been tested to evaluate w_e and αw_p (three tests were realized for each ligament length l_0 chosen).

Results and discussion

Typical stress–strain curves from tensile tests on PET and two PET coating specimens are shown in Fig. 2.

The investigated materials exhibit a ductile behaviour with similar tensile energy to fracture ranging from 7 to about 11 kJ/m^3 (Table 2). These results suggest that the

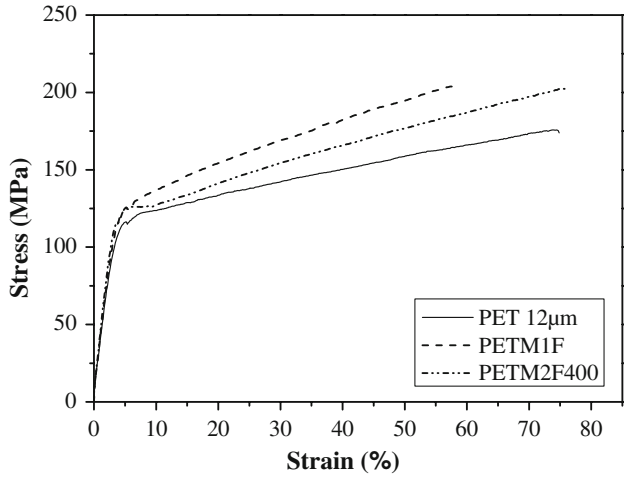

Fig. 2 Tensile stress versus strain curves of the PET and PET-metallized films of 12 µm thickness loaded in machine direction

tensile test can hardly be used to characterize fracture performance of multilayers materials and that this parameter obtained from the tensile test is not enough discriminant.

Figure 3a presents the load–displacement curves of the DENT specimens with various ligament lengths of the PET 12 µm specimens metallized on one side with 20 nm of aluminium tested in the longitudinal direction. The ligament lengths corresponding to the crack propagation initiation have been indicated on the curves. It was observed that the maximum load and the rupture extension increase with ligament length. Nevertheless, a similar shape of the load versus displacement was observed for all the polymer–metal materials, independently of the ligament length. In the composites studied, crack propagation takes place after yielding of the polymer. Indeed, these curves display a maximum which corresponds to blunting due to complete ligament yielding. Beyond this maximum, a slow load decrease indicates slow stable crack propagation into yielded ligament, perpendicularly to the load direction [5].

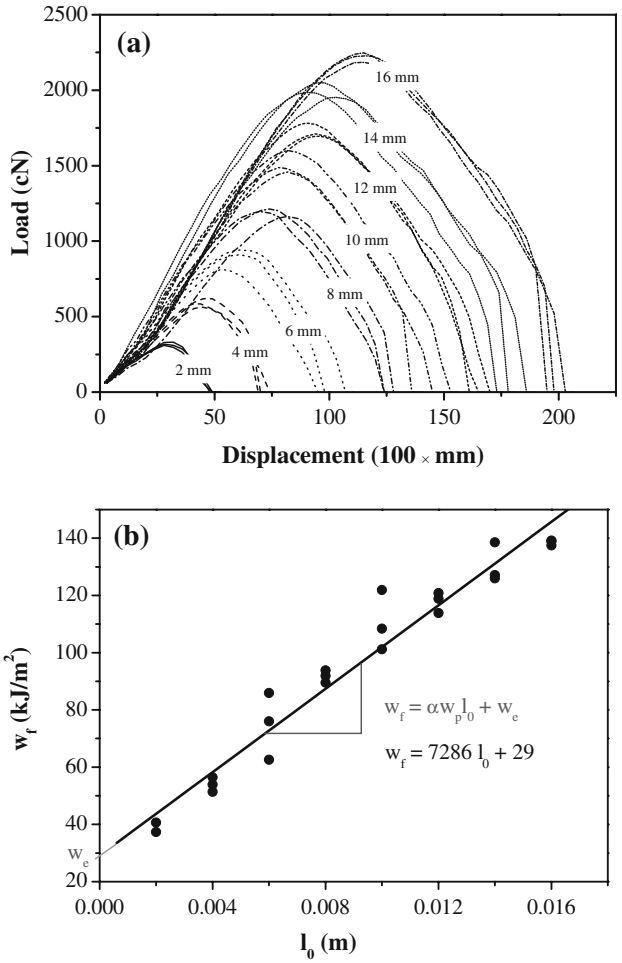

Fig. 3 **a** Load–displacement curves of PETM2F400 film with various ligament lengths (2–16 mm). **b** Variation of the specific work of fracture versus ligament length for separation of the EWF of PETM2F400 film

The method to determine the specific work of fracture requires calculation of the total energy divided by the initial ligament area. Figure 3b depicts the work of fracture w_f as a function of the ligament length l_0 curves for PET

Table 2 Results for the polymer–metal films

Films	Aluminium thickness (nm)	Tensile energy to break (kJ/m^3)	w_e (kJ/m^2)	Δw_e (kJ/m^2)	αw_p (MJ/m^3)	Crystallinity (%)
PETM1FRO	30	9.5	20	10	6.8	38
PETTCF	20	10.4	21	8	6	35
J201	20	10.1	21	9	8.2	36
PET 12 µm	–	11.4	24	11	8.6	37
J231	20	8.1	24	8	8.2	38
PETM1F	20	9.3	28	6	7.9	36
PETM2F400	2 × 40	11.4	29	7	7.3	33
PETM1F400	40	7	32	7	7.7	36
PETM1F800	80	10.8	32	8	7.5	32

Δw_e standard deviation

composite metallized on two sides; as expected, a linear correlation is observed. The specific EWF is obtained by extrapolating the straight line to zero ligament length. The non-essential part, or plastic work term (αw_p), was also obtained from the slope of the linear relation of w_f versus ligament length. This analysis was performed for all the composites listed in Table 1 and the corresponding results are reported in Table 2. The accuracy of the measure is also given; it is worth noting that the obtained regression coefficients (R^2) are satisfactory (above 90%).

While the curves for the metallized films are smooth, the beginning of the loading curve for the reference PET ($l_0 > 4$ mm) presents a "pop-in stage", which is not present for the composite layers (Fig. 4). This reflects a striction which is the result of a localized plastic flow for the PET, and it is likely that a metallic coating on the substrate prevents the necking and limits this effect. The EWF for PET was determined by two methods which consider or not the striction (Fig. 5). The resulting values for the essential specific work of fracture of the PET 12 μm with an extrapolation accounting or not for the striction are of 29 and 28 kJ/m^2, respectively. The difference would thus be considered as not significant, and the fracture mode as independent of the striction.

In the case of the polymer–metal composites, the largest value of the essential specific work of fracture is associated to the films having the thickest aluminium layer. Despite the large experimental uncertainties, the effect is significant. As most of the dissipation should take place inside the polymer, this result is quite surprising because all the specimens were realized from the same batch of PET 12 μm. The simplest possible explanation is that the treatments applied during the metallization process may be responsible for structural evolutions in the polymer layer.

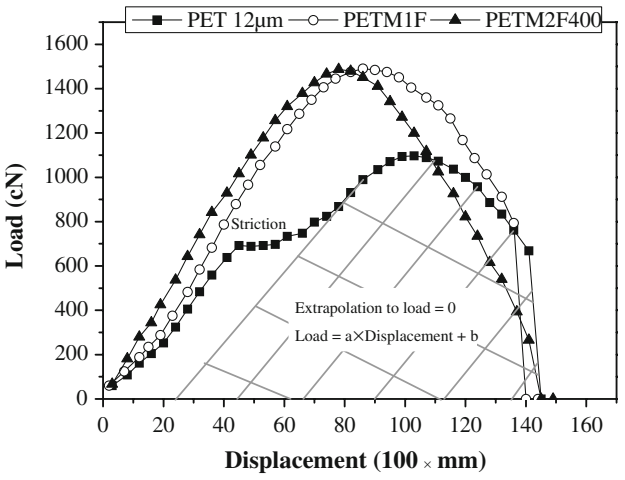

Fig. 4 Typical DENT load–displacement curve for PET reference and two PET-metallized specimens. Nominal ligament length = 10 mm. The relevant quantity is the area under the curve

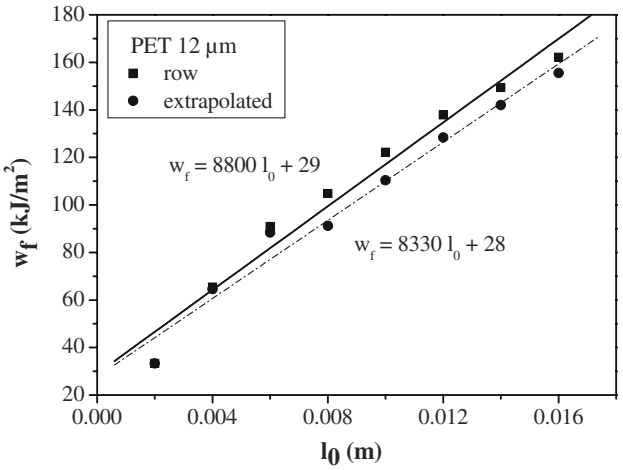

Fig. 5 Total specific work of fracture (w_f) versus ligament length (l_0) from the PET specimens calculated with or without striction

In order to test this hypothesis, differential scanning calorimetry (DSC) experiments were carried out to explore possible structural evolutions and to measure the polymer layer crystallinity. A thermogram comparing PET and PET composite metallized on two sides is shown in Fig. 6. This thermogram focuses on the melting peak which reveals the amount of crystallinity.

The melting peak of the PET film starts at 230 °C, whereas the melting peak of the composite is shifted towards lower temperature and presents a smaller area. Both observations indicate a larger crystalline fraction in the polymeric film after the metallization process has taken place.

The fraction of crystalline material, calculated from the apparent enthalpy of fusion, is reported in Table 2. It is observed that the crystallinity systematically decreases when the aluminium thickness deposited on the PET substrate increases. The variations obtained on the specific

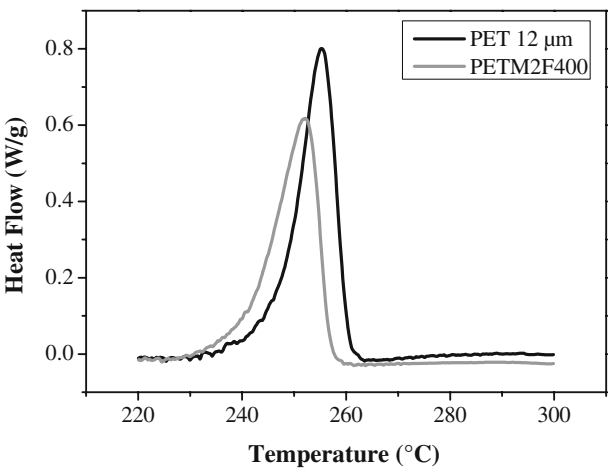

Fig. 6 DSC analyses of PET reference and PET metallized showing the thermal transitions versus temperature

essential work of fracture (w_e) values and on the crystallinities could be attributed to two possible effects. The first is associated to the geometry of the composites, namely the number of layers and the thickness of metal. It is worth noticing that a chemical treatment leads to an increase in thickness of 0.3 μm for the 12 μm PET. This variation is considered as negligible. The second concerns the intrinsic material properties which may be modified as an effect of the different treatment. Figure 7 shows a correlation between the crystallinity and the EWF. The crystallinity is a first-order parameter in the work of fracture: a change in crystallinity by 5% corresponds to a decrease by around 10 kJ/m^2 ($\sim$30%) in the EWF.

Figure 8 presents the method employed for calculating theoretical values for w_e in order to evaluate the influence of each parameter. Multiple linear regression attempts to model the relationship between two explanatory variables and a response variable by fitting a linear equation to observed data. Every value of the independent variable x (aluminium thickness) is associated with a value of the dependent variable y (crystallinity). It appears that aluminium thickness and crystallinity are correlated. In fact, (i) w_e increase with aluminium thickness (Fig. 8a), (ii) w_e decreases when crystallinity increases (Fig. 8b), (iii) crystallinity increases when aluminium thickness decreases.

In order to assess the effect of other parameters such as metallization thickness and PET surface treatments, Figs. 9 and 10 show, for films with an amount of crystallinity of 35 ± 5%, the results for different composites, namely PETM1F400, PETM1F, J201 and PETTCF. From Fig. 9, it appears that: (i) an increase in the quantity of metal deposited on the PET increases the cracking resistance of the material; (ii) a treatment of the PET surface tends to

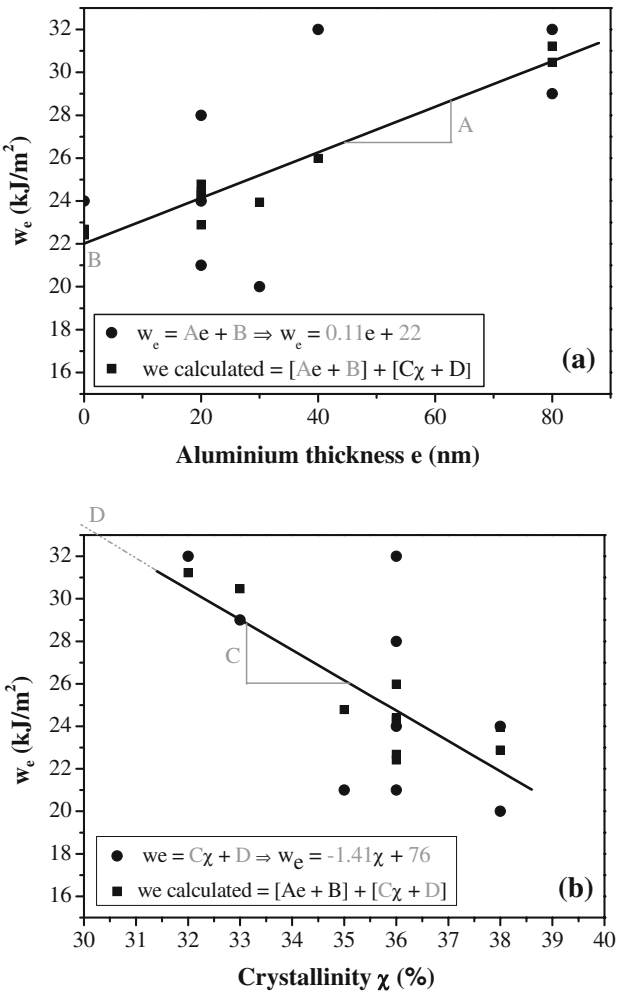

Fig. 8 Correlation between the amount of crystallinity of the polymer layer, the aluminium layer and the EWF. *A*, *B* and *C*, *D* were simultaneously determinated from (**a**) and (**b**), respectively

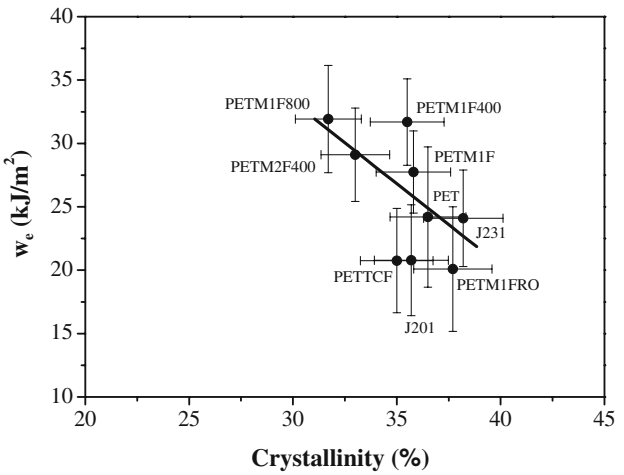

Fig. 7 Correlation between the crystallinity of the polymer layer and the EWF

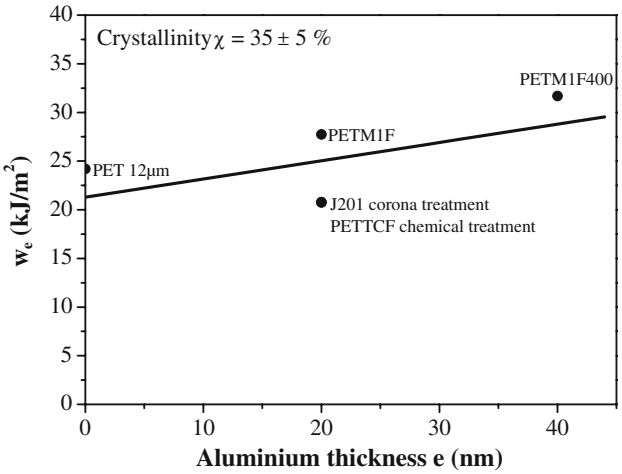

Fig. 9 Results of w_e versus aluminium thickness for materials having the same crystallinity

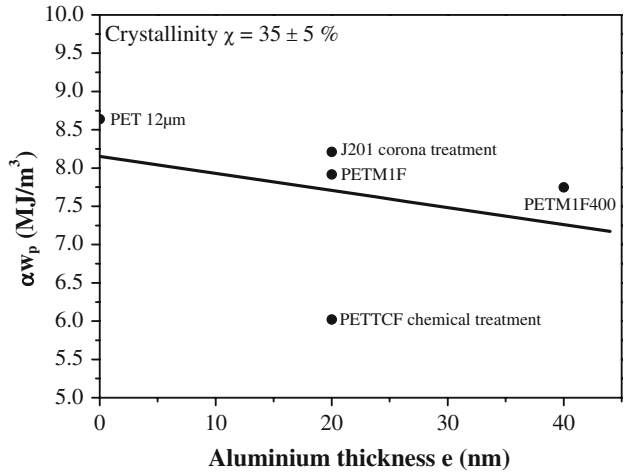

Fig. 10 Results of αw_p versus aluminium thickness for materials having the same crystallinity

decrease toughness. In addition, Fig. 10 shows that aluminium thickness and treatments play a significant role on the plastic work; αw_p decreases clearly with the thickness and with the application of chemical treatment on the PET surface.

Conclusion

The EWF method is known to be a discriminant test to evaluate the fracture behaviour of ductile materials. The EWF procedure was successfully applied to the multilayers polymer–metallic films. It was shown that the amount of crystallinity, which can be modified during the metallization process, is the first-order microstructural parameter governing the specific EWF. Whereas the fracture toughness of material decreases when the amount of crystallinity increases, the brittle phase becomes more important. At second-order, for a given crystallinity, increasing the metal thickness increases the resistance to fracture, while the application of a surface treatment on PET films decreases it. Thermal history linked to metallization process could qualitatively explain the evolution of crystallinity. In fact, other results, not presented here, showed that film's crystallinity decreases about of 20 to 30% between first and second heating. It is worth noticing that first heating considers fabrication process, whereas second heating reveals intrinsic properties of materials.

Acknowledgements This study was partly financed by ANR (French Agence Nationale de la Recherche) through the BARISOL Prebat Project overviewed by ADEME (Agence De l'Environnement et de la Maîtrise de l'Energie, French Agency for Environment and Energy Management). We specially thank Rexor Company for important contribution to the set-up of the film fabrication.

References

1. Broberg KB (1975) J Mech Phys Solids 23:215
2. Brunner S, Gasser P, Simmler H, Wakili K (2006) Surf Coat Technol 200:5908
3. Chehab B, Brechet Y, Glez J, Jacques P, Mithieux J, Véron M, Pardoen T (2006) Scr Mater 55:999
4. Cotterell B, Reddel JK (1977) Int J Fract 13:267
5. Fayolle B, Audouin L, Verdu J (2003) Polymer 44:2773
6. Fung LR (2005) Polym Test 24:863
7. Hu S, Hiltner A, Baer E (2005) J Appl Polym Sci 98:1629
8. IEA Annex 39 (2005) High performance thermal insulation in building and building systems. Final report, www.vip-bau.ch
9. Kocsis J, Czigany T (1996) Polymer 37:2433
10. Kong Y, Hay J (2002) Polymer 43:3873
11. Lach R, Schneider K, Weidisch R, Janke A, Knoll K (2005) Eur Polym J 41:383
12. Marchal Y, Delannay F, Froyen L (1996) Scr Mater 35:193
13. Maspoch M, Hénault D, Velasco J, Santana O (2000) Polym Test 19:559
14. Moosheimer U, Bichler C (1999) Surf Coat Technol 116–119:812